Three-Dimensional Imaging Using a Frequency-Domain Synthetic Aperture Focusing Technique

L. J. Busse, *Member, IEEE*

Abstract—**A frequency domain method for implementing the synthetic aperture focusing technique is developed and demonstrated using computer simulation. As presented, the method is well suited to reconstructing ultrasonic reflectivity over a volumetric region of space using measurements made over an adjacent two-dimensional (2-D) aperture. Extensive use is made of both one- and two-dimensional Fourier transformations to perform the required temporal and spatial correlation required by the technique, making the method well suited to general purpose computing hardware. Results are presented demonstrating both the lateral and axial resolution achieved by the method. The effect of limiting the reconstruction bandwidth is also demonstrated.**

I. Introduction

THE SYNTHETIC aperture focusing technique (SAFT) has long been recognized as a method well suited for generating high resolution images, over a large depth of field using ultrasound [1]. SAFT has been most often applied in the field of nondestructive evaluation [2], [3] for detection and characterization of defects in thick metal structures, however, as two-dimensional (2-D) imaging arrays for medical imaging are developed [4], it may also be a useful tools for researchers in medical imaging.

The method coherently combines pulse–echo measurements made at a multitude of transmitter/receiver locations to form a map of the ultrasonic reflectivity of the region being insonified. SAFT takes advantage of both spatial and temporal correlations to enhance the resolution and the signal-to-noise ratio of the resultant images. The multiple transmit/receive locations have been realized either by using a single transducer, mechanically scanned in a one- or two-dimensional aperture [5] or by using a linear array of transducer elements [6]–[9]. The previous implementations of the SAFT have relied on a "delay and sum," time-domain processing strategy that was shown to be quite time consuming on general purpose computing equipment [10]. For efficient implementation, SAFT has required either special purpose computing hardware [11] or beam forming hardware [6]–[9]. Historically, synthetic aperture imaging systems were developed in the field of radar mapping and surveillance. In the early 1970's, the first ultrasonic SAFT systems were assembled in direct analogy to the radar systems [1]. Data were originally recorded in an analog fashion (on film) and processed optically.

Manuscript received June 13, 1991; revised and accepted September 10, 1991. This work was supported by DHHS NIH Grant R43 HL44230-01.

The author is with the TETRAD Corporation, 12741 E. Caley Ave. #126, Englewood, CO 80111.

IEEE Log Number 9105554.

The first digital implementation of SAFT using computers for the data processing, soon followed. This technology has since been applied in the inspection of thick section metal components found in the nuclear industry [11], [12] and in the aerospace industry [6]–[9].

These original SAFT systems, made use of a time delay algorithm (sometimes called the delay-and-sum method) for simulating the required lens effect. This approach, while physically understandable, was cumbersome for implementing on a general-purpose computer system. Much effort has been expended to adapt this delay and sum algorithm so that it could be implemented upon specially designed real-time SAFT processors [11].

In this paper, a frequency-domain form of the SAFT (FD-SAFT) algorithm is presented. In the past, a number of frequency domain approaches have been taken to synthetic aperture imaging, but most have concentrated on producing 2-D images in a B-scan [13]–[16]. The method presented here is similar to that of Teo and Reid [17] but is unique in that it uses broadband pulses for data collection and it is specifically aimed at producing three-dimensional (3-D) reconstructions of the inspected volume. FD-SAFT is an extension of the angular spectrum technique [18], [19] of scalar diffraction theory for back-propagating a measured field pattern from the measurement plane to any other parallel plane. The FD-SAFT algorithm makes use of both temporal and spatial Fourier transforms to efficiently perform the correlations required for SAFT imaging in the frequency domain. Because the algorithm relies heavily on Fourier transforms, it can be efficiently implemented using more commonly available computer hardware such as array processors, accelerator cards, or DSP chips. To underscore the efficiency, all of the simulation results presented in this paper were obtained using FFT software [20] and a commonly available personal computer.[1]

II. Theory

The frequency domain form of the synthetic aperture focusing technique (FD-SAFT) to be described is based upon a mathematical analysis technique, known as angular spectrum decomposition [18], [19]. In this section the narrow band (single frequency) version of this technique will be briefly presented and then extended to the case of broadband (pulsed) image reconstruction techniques. The theory presented assumes that data are collected using a series of measurements from a "point-like" sensor. Such a sensor might consist of

[1] For example, a microcomputer based on the Intel 80386/387.

an array of omnidirectional transducers or a single transducer scanned over a planar receiver aperture.

A. Narrow Band Version

Let $U(x, y, 0)$ represent the complex (real and imaginary) acoustic pressure field measured over a 2-D aperture (characterized by x, y) at the plane $z = 0$. By 2-D Fourier transformation this pressure field can be represented by its angular spectrum, a series of components $A(K_x, K_y; 0)$

$$A(K_x, K_y; 0) = \iint_{-\infty}^{\infty} U(x, y : 0) \exp\left[i(xK_x + yK_y)\right] dx\, dy \tag{1}$$

where $K_x = \alpha k$, $K_y = \beta k$, K_x and K_y are called spatial wavenumbers, k is the ultrasonic wavevector (ω/v); α and β are directly interpretable as the direction cosines of plane wave components. The effect of the 2-D Fourier transformation is to break the measured field distribution U into a series of plane wave components each propagating at a known angle specified by (α, β). Conversely, the inverse transformation

$$U(x, y; 0) = \frac{1}{2\pi} \int \int_{-\infty}^{\infty} A(K_x, K_y; 0) \cdot \exp\left[-i(xK_x + yK_y)\right] dK_x\, dK_y \tag{2}$$

shows how the measured field is composed of its angular spectrum. In addition to the above equation, U must also satisfy the Helmholtz equation

$$\nabla^2 U + k^2 U = 0 \tag{3}$$

in all regions of space free from sources (or sinks) of ultrasound. Substitution of the above equation into (2) and interchange of the order of differentiation and integration leads to a second-order homogeneous differential equation with the following solution:

$$\begin{aligned} A(K_x, K_y; z) &= A_0(K_x, K_y; 0) \\ &\quad \exp\left(iskz\left(1 - (K_x/sk)^2 - (K_y/sk)^2\right)^{1/2}\right) \\ &= A_0(K_x, K_y; 0) B(z, \omega) \end{aligned} \tag{4}$$

where $s = 1$ for a fixed transmitter/scanned receiver and $s = 2$ for a simultaneously scanned transmitter/receiver [21], [22]. In other words, the effect of wave propagation from a plane $z = 0$ to another arbitrary plane z, can be determined by simply adjusting the relative phase of each of the plane wave components. The complex exponential term in the above equation is sometimes called the backward wave propagator. This propagator, designated as B, is an explicit function of frequency ω and the distance of propagation z and can be characterized as a linear, dispersive spatial filter. Following application of this filter, the ultrasonic field at the new plane can be calculated as the 2-D Fourier transform of the A:

$$U(x, y; z) = \frac{1}{2\pi} \iint_{-\infty}^{\infty} A(K_x, K_y; z) \exp\left[-i(xK_x + yK_y)\right] dK_x\, dK_y \tag{5}$$

This result is well known and is an extensively applied image reconstruction algorithm in the area of acoustic holography where measurements are generally made at a single frequency (or a very limited range of frequencies). Single frequency acoustic holography provides diffraction limited lateral resolution, however, axial or depth resolution is poor.

B. Broadband Version

A pulsed or broadband version of this imaging procedure can be developed by applying the above imaging procedure to each frequency component of the pulsed waveform. Let $u(x, y; 0, t)$ represent the set of complex waveforms recorded by a point receiver as it is scanned in the plane located at $z = 0$. A Fourier transform with respect to time can then be used to break these waveforms into a set of complex pressure fields, each representing a discrete frequency ω:

$$U(x, y; 0, \omega) = \int_{-\infty}^{\infty} U(x, y; 0, t) \exp\left(i\omega t\right) dt,\ t_{\text{ref}} = 0 \tag{6}$$

where the reference time, $t_{\text{ref}} = 0$, is meant to indicate that all waveforms are referenced to the time at which the transmitter is fired. Subsequent application of a 2-D Fourier transform to each frequency component

$$A(K_x, K_y; 0, \omega) = \iint_{-\infty}^{\infty} U(x, y; 0, \omega) \exp\left[i(xK_x + yK_y)\right] dx\, d$$

(7)

yields a set of angular spectra that can be used to completely characterize the recorded pulsed pressure field at $z = 0$. The angular spectrum can be used to calculate a series of complex images at any other plane z by application of the appropriate filter function. To calculate the complex pressure fields with respect to a new plane z:

$$\begin{aligned} A(K_x, K_{y;z,\omega}) &= A_0(K_x, K_y; 0, \omega) B(z, \omega) \\ \text{where } B(z, \omega) &= \exp\left(iskzC\right) \\ C &= \left(1 - (K_x/sk)^2 - (K_y/sk)^2\right)^{1/2} \\ k &= \omega/\nu. \end{aligned} \tag{8}$$

The dimensionality of this new angular spectrum must now be reduced in order to form the processed image.

The first method to be considered is to simply invert the processes that were used to form A. A series of inverse 2-D Fourier transforms can be applied

$$U(x, y; z, \omega) = \frac{1}{2\pi} \iint_{-\infty}^{\infty} A(K_x, K_y; z, \omega) \exp\left[-i(xK_x + yK_y)\right] dK_x\, dK_y \tag{9}$$

to form a series of single frequency images. The images can then be integrated

$$< U(x, y; z) > = \int_{-\infty}^{\infty} U(x, y; z, \omega)\, d\omega \tag{10}$$

to form the equivalent broadband image at the plane z.

In practice, however, the function U is measured by sampling the receive aperture at fixed intervals, δx and δy.

Physically, this fixed sampling makes the spatial wavenumbers independent of the ultrasonic frequency since the spatial wavenumbers are inversely proportional to the spatial sampling intervals. Noting these sampled wavenumbers as K'_x and K'_y, (9) and (10) can be rewritten as (11). By interchanging the order of spatial and temporal integrations, averaging over frequency ω can be accomplished in the spatial frequency domain. The average image $< U(x,y;z)>$ is therefore formed with a single inverse 2-D transform rather than one transform for each frequency component as in (9).

To summarize, the broadband algorithm consists of the following steps:

1) Take the Fourier transform of each waveform,
2) Select the frequencies to be used for reconstruction and store a series of complex pressure fields, $U(x,y;0,\omega)$,
3) Take the spatial 2-D Fourier transform of each of these pressure fields to form the angular spectrum at each frequency, $A(K'_x,K'_y;0,\omega)$,
4) Apply the propagator function $B(z,\omega)$ to each angular spectrum to transform it to the plane of interest, $A(K'_x,K'_y;z,\omega)$,
5) Average these components over frequency ω to form $< A(K'_x,K'_y;z) >$, and
6) Finally, take the magnitude of the inverse Fourier transform of this averaged angular spectrum to form an image of the plane $z, | < U(x,y;z) > |$.

III. Methods

To test the FD-SAFT algorithm as outlined in the previous section, a computer program was written to generate (simulate) the set of waveforms that would be observed by an omnidirectional transmit/receiver transducer when it is scanned in a raster fashion over a square receiver aperture. The receiver aperture was sampled at $\lambda/2$, where λ is defined by the center frequency (v/F_{center}), in both the x and y dimensions. The full aperture L was 32λ at the center frequency. (This choice of sampling could conceivably lead to undersampling of high spatial frequency components for temporal frequencies higher than F_{center}. The simulations that follow, however, were performed with reflectors located at sufficient range so that no undersampling would occur.) The program was written to allow an arbitrary number of point scatters to be located in the volume of interest. Data from this computer program were recorded for subsequent processing. Fig. 1 illustrates the geometry used for these simulations. A second computer program was written to implement the FD-SAFT reconstruction algorithm. Standard floating point FFT software

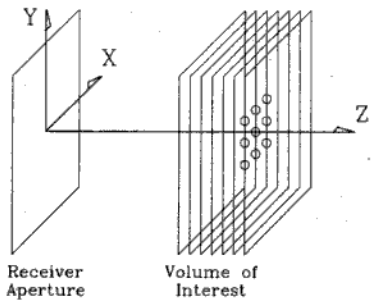

Fig. 1. Illustration of the geometry associated with FD-SAFT. Data is collected by sampling the receiver aperture and a 3-D reconstruction is formed by imaging at multiple planes in the volume of interest.

[20] and ANSI-standard C compilers[2] were used to implement both programs on a personal computer.

To illustrate the effects of the multifrequency approach on axial and lateral resolution a data set was generated for a single point reflector located on axis at a range equal to 2 aperture widths (64λ) from the receive aperture (i.e., a normalized range of 2). The time and frequency domain characteristics of the pulse used for this simulation are illustrated in Fig. 2. The pulse was a Hamming weighted sinusoid, of three cycles duration sampled at 5 points per cycle. A set of 64×64, 512 point waveforms (A-scans), quantized to 8-bit accuracy, were generated as used as input for the FD-SAFT algorithm.

Fig. 3 shows the result of this calculation in terms of the point-spread-function (PSF) for two extreme cases; panel A shows the image of the single point reflector when only a single frequency component at the center of the pulse is used for the reconstruction and panel B shows the image of the same point when 31 frequency components, symmetrically spaced about the pulse center frequency, were included in the reconstruction. The full 64×64 aperture is displayed ($-L/2 < x,y < L/2$) in these plots and the data is plotted on a linear scale. The lateral resolution is comparable for these two PSF's however the effects of increased clutter level is more apparent for the single frequency image. Increased clutter is probably a result of quantization error since only simulated 8-bit data were used.

Fig. 4 shows the results of the FD-SAFT algorithm in terms of axial resolution. The results of four different reconstruction procedures are summarized in this figure. Each reconstruction was performed for a series of 21 planes located at normalized ranges from 1.6 to 2.4. Reconstructions were made using 1,

[2]Depending on memory requirements, different compilers were used: 1) Turbo-C++ compiler and linker, from Borland International, Scotts Valley, CA and 2) NDP C-386 from Microway, Inc. Kingston, MA, used with 386|ASM/Link/DOS Extender from Phar Lap Software, Inc., Cambridge, MA.

$$< U(x,y;z) > = \frac{1}{2\pi}\int_{-\infty}^{\infty}\left\{\int\int_{-\infty}^{\infty} A(K'_x,K'_y;z,\omega)\exp\left[-i(xK'_x+yK'_y)\right]\,dK'_x\,dK'_y\right\}d\omega$$
$$= \frac{1}{2\pi}\int_{-\infty}^{\infty}\left\{\int_{-\infty}^{\infty} A(K'_x,K'_y;z,\omega)\,d\omega\right\}\exp\left[-i(xK'_x+yK'_y)\right]\,dK'_x\,dK'_y. \quad (11)$$

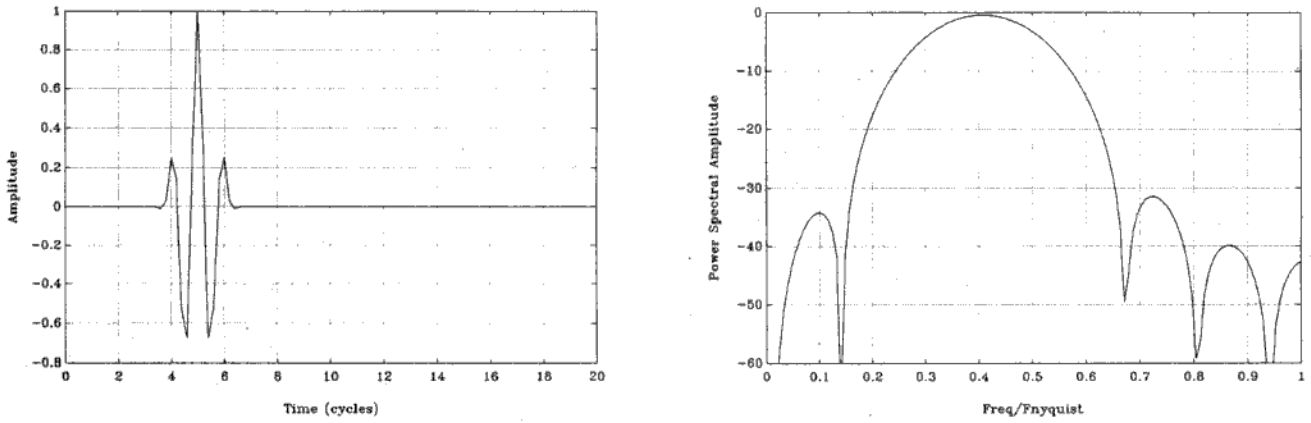

(a) (b)

Fig. 2. Shows the time (a) and frequency (b) domain signals used in the imaging simulations.

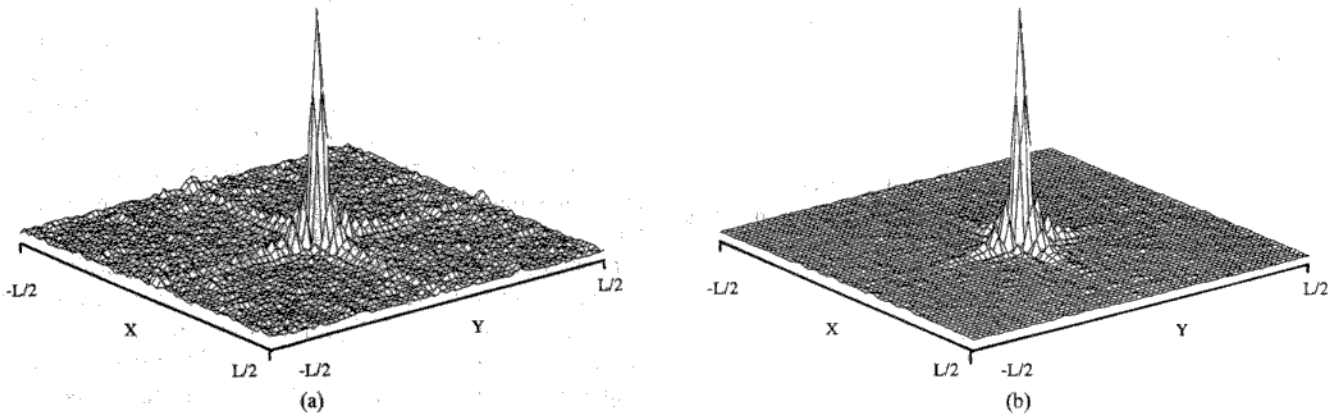

(a) (b)

Fig. 3. Shows the image of a single point reflector (point spread function) located at the center of the aperture and at a normalized range of 2. This corresponds to an x,y aperture L of 32 λ_{center} at a range z of 64 λ_{center}. Panel A shows PSF over the full aperture when only the center frequency of the pulse was used and panel B shows the PSF obtained when 31 frequency components of the pulse were used. The vertical scale is linear.

11, 21, and 31 frequency components. The effect of increased bandwidth on axial resolution is clearly depicted. When one frequency component is used, the axial resolution is basically only that provided by the focal properties (depth of field) of the aperture. As the number of frequency components is increased to 31, the axial resolution becomes comparable to pulse length used for the simulation, (in this case, 1.6 cycles of the center frequency is equivalent to a normalized range of 0.05). In other words, depth resolution is not sacrificed by using the frequency domain approach as long as a sufficient number of frequencies are included.

Fig. 5 depicts a grey-scale image of a more complicated set of point reflectors located at a normalized range of 2 and arranged as follows: in the center of the image is a 3×3 set of points separated by 2 λ; in quadrant 1, a 3×3 set separated by λ; in quadrant 2, a 3×3 set separated by 2 λ; in quadrant 3, a 3×3 set separated by 3 λ; and in quadrant 4, a 3×3 set separated by 4 λ. This image was reconstructed using 31 frequency components, a 32-λ aperture, at a range of 64 λ, and is displayed with a linear gray scale. From 0–10% of full scale is shown in black, a 64 level linear gray scale is used to represent values from 10% to 100% of full scale. The image

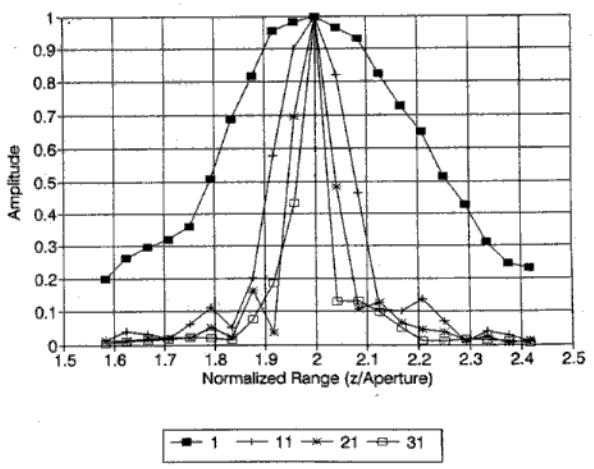

Fig. 4. Plot showing the effect of the reconstruction bandwidth upon the axial resolution. The four curves show the axial response for a single point reflector at a normalized range of 2 when 1 (■), 11 (+), 21(*), and 31(□) frequency components are used.

demonstrates that the resolving power of FD-SAFT near the edges of the aperture is quite comparable to that observed at the center of the aperture.

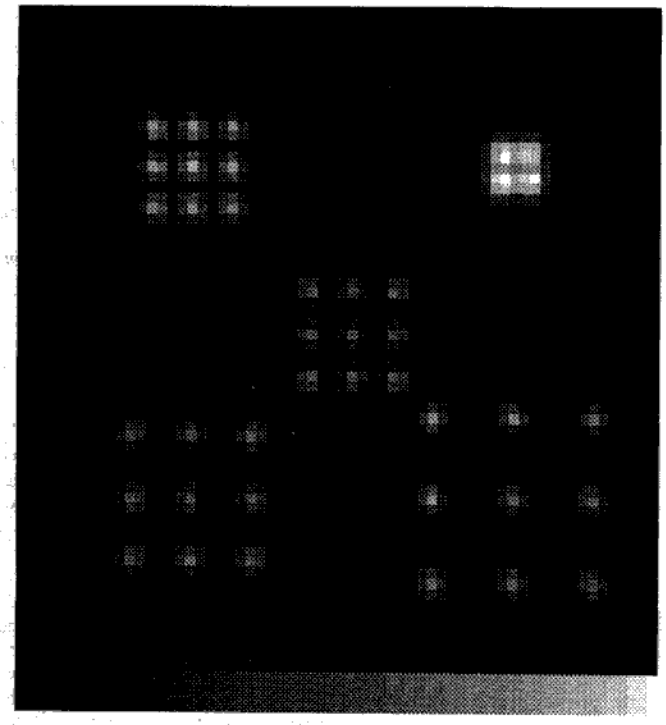

Fig. 5. Imaging of five groups of 9-point reflectors made at a normalized range of 2. This corresponds to an x, y aperture of 32 λ_{center} at a range of 64 λ_{center}. The image, shown over the full x, y aperture, was made using 31 frequency components and is displayed using a linear, 64 level gray scale.

IV. Conclusion

In this paper, a theoretical description and demonstration of a frequency domain, synthetic aperture imaging method has been presented. The method, which is based on the angular spectrum method of wavefront analysis, makes extensive use of temporal and spatial Fourier transforms to implement the correlations required for synthetic aperture imaging. The method allows data collected over a 2-D aperture to be formed into a 3-D representation of ultrasonic reflectivity.

Simulation results have been presented for the case of a simultaneously scanned transmitter/receiver. The results indicate that diffraction limited lateral resolution can be achieved and that the axial resolution is inversely related to the bandwidth of the reconstruction. In practice, the lateral and axial resolution will most likely be limited by actual properties of the transducer or sensor used to collect the data: the directivity pattern of the transmitter/receiver will limit lateral resolution and pulse response or bandwidth will limit axial resolution.

During the course of these simulations it was found that the most time consuming process was the large number of time domain (one-dimensional (1-D)) FFT's that are required; for these simulations, 4096 1-D FFT's for each simulation. When implemented in hardware, these FFT's would best be performed as part of the data collection process. Signal processing hardware can perform the necessary calculations at rates comparable to the pulse repetition frequencies used for ultrasonic imaging. Implementing the FFT's as part of the data collection process would also reduce the data storage and handling requirements since only a predetermined (limited) number of Fourier coefficients would have to be retained rather than an entire waveform record.

For coherent phasing of multifrequency reconstructions, the recorded A-scans have to be time referenced, so that $t = 0$ corresponds to the time at which the transmitter is fired. In practice, however, it is desirable to limit the recorded time window and to start A-scan recording at a later time. In these situations, for proper phasing the reconstructed components, it is necessary to either apply a phase compensation factor either in the time-domain before the 1-D FFT's or in the frequency-domain after the 1-D FFT's. In the time domain, the required time operation is to apply a shift so that the first recorded point falls on a point that corresponds to an integer times the number of points recorded per waveform.

The next most time consuming step of the process is calculating the backward wave propagator for each plane in a 3-D reconstruction. FD-SAFT, as presented, requires the backward wave propagator to be calculated and applied at each depth where a reconstruction is to be performed. This is a rather heavy computational load since it involves a 2-D transcendental function that must be performed at every depth and at every frequency. Some reduction in the computational effort might be gained by considering the physical function of the backward wave propagator and by examining the results presented in Fig. 4.

In a sense, the propagator is a correlation function that has the right focal properties for the frequency and depth of interest. A plot of the propagator (not shown) reveals a ring pattern that is basically a Fresnel zone plate, or lens that provides the phase shifts necessary at the frequency ω for focal plane response at z. Such a lens has associated with it a range of z values over which an acceptable focal response can be achieved (as is shown in Fig. 4 for the one frequency reconstruction result). The range, known as the depth of field, should allow the number of propagators needed for the reconstruction to be significantly reduced.

By breaking the total range of depths into bands (or focal zones) the computational load can be significantly reduced. The width of each of these bands should be determined by the optical element that limits the overall depth of field at a single frequency; either the scanned aperture or the directivity pattern of the sensor. (Previous analysis of SAFT resolution indicates that receiver directivity patterns are the limiting element in most practical situations [3].)

As a final comment, the methods presented in this paper were restricted to planar receiver apertures and a scanned transmit/receive sensor element. It is possible to extend this procedure to other sensor configurations such as fixed transmitter/scanned receiver geometries or even sparse array geometries where a limited number of transmit/receive locations are used for data collection.

References

[1] D. W. Prine, "Synthetic aperture ultrasonic imaging," in *Proc. Eng. Appl. Holography Symp.*, vol. 287, SPIE, 1972.

[2] J. A. Seydel, "Ultrasonic synthetic aperture focusing techniques in NDT," in *Research Techniques in Nondestructive Testing*, vol. 6, R.S. Sharpe, Ed. New York: Academic, 1983.

[3] L. J. Busse, H. D. Collins, and S. R. Doctor, "Review and discussion of the development of synthetic aperture focusing technique for ultrasonic testing (SAFT-UT)," NUREG/CR-3625, 1984.
[4] S. W. Smith, H. G. Pavy, Jr., and O. T. von Ramm, "High-speed ultrasound volumetric imaging system—Part I: Transducer design and beam steering," *IEEE Trans. Ultrason. Ferroelec. Freq. Contr.*, vol. UFFC-38, no. 2, pp. 100–108, 1991.
[5] V. M. Schmitz, W. Muller, and G. Schafer, "A new ultrasonic imaging system," *Materials Eval.*, vol. 40, 1982.
[6] P. D. Corl, G. S. Kino, C. S. DeSilets, and P.M. Grant, "A digital synthetic focus acoustic imaging system," in *Acoustical Imaging*, vol. 8, A.F. Metherell, Ed. New York: Plenum, 1980.
[7] P. D. Corl and G. S. Kino, "A real-time synthetic aperture imaging system," in *Acoustical Imaging*, vol. 9, K. Y. Wang, Ed. New York: Plenum, 1980.
[8] G. S. Kino, P. D. Corl, S. Bennett, and K. Peterson, "Real time synthetic aperture imaging system," *IEEE Symp. Proc.*, 1980.
[9] D. K. Petersen, S. D. Bennett, and G. S. Kino, "Real time digital imaging," *IEEE Symp. Proc.*, 1981.
[10] S. Ganapathy, W. S. Wu, and B. Schmult, "Analysis and design considerations for a real-time system for nondestructive evaluation in the nuclear industry," *Ultrason.* vol. 20, 1982.
[11] T. E. Hall, L. D. Reid, and S. R. Doctor, "SAFT-UT (Synthetic aperture focusing technique for ultrasonic testing) real-time inspection system: Operational principles and implementation," 1988.
[12] Y. Ozaki, H. Sumitani, T. Tomoda, and M. Tanaka, "A new system for real-time synthetic aperture ultrasonic imaging," *IEEE Trans. Ultrason., Ferroelec., Freq. Contr.*. vol. 35, pp. 828–838, 1988.
[13] H. Ermert, and R. Karg, "Multifrequency acoustical holography," *IEEE Trans. Sonics Ultrason.*, vol. SU-26, p. 279, 1979.
[14] B. P. Hildebrand, T. J. Davis, A. J. Boland, and R. L. Silta, "A portable digital ultrasonic holography system for imaging flaws in heavy section materials," *IEEE Trans. Sonics Ultrason.*, vol. SU-31, p. 287, 1984.
[15] K. Nagai "Multifrequency acoustical holography using a narrow pulse," *IEEE Trans. Sonics Ultrason.*, vol. SU-31, p. 151, 1984.
[16] ——, "A new synthetic-aperture focusing method for ultrasonic b-scan imaging by Fourier transform," *IEEE Trans. Sonics Ultrason.*, vol. SU-32, p. 531, 1985.
[17] T. J. Teo and J. M. Reid, "Multifrequency holography using backprojection," *Ultrason. Imaging*, vol. 8, pp. 213–224, 1986.
[18] J. W. Goodman, *Introduction to Fourier Optics*. New York: McGraw-Hill, 1968, ch. 3.
[19] E. G. Williams and J. D. Maynard, "Numerical evaluation of the Rayleigh integral for planar radiators using the FFT," *J. Acoust. Soc. Amer.*, vol. 72, pp. 2020–2030, 1982.
[20] W. H. Press, B. P. Flannery, S. A. Teukolsky, and W. T. Vetterling, "Numerical recipes," in *C: The Art Of Scientific Computing*. Cambridge, UK: Cambridge Univ. Press, 1988, ch. 12.
[21] H. D. Collins, R. P. Gribble, V. L. Crow, R. W. Gilbert, and R. L. Wilson, "The design, construction and demonstration of a prototype digital processor for a production prototype pressure vessel imaging inspection system," EPRI RP606-8, pp. 1–12, 1983.
[22] B. P. Hildebrand and K. A. Haines, "Holography by scanning," *J. Opt. Soc. Amer.*, vol. 59, 1969.

L. J. Busse (M'80) was born in Covington, KY, on June 16, 1951. He received the B.A. degree in physics in 1973 from Thomas More College, Covington, KY, and the M.A. and Ph.D. degrees in physics in 1975 and 1979, respectively, from Washington University, St. Louis, MO.

He worked at Battelle-Pacific Northwest Laboratories until 1984 where his research interests include transducer design and the development of ultrasound methods for materials characterization and imaging as it applies to nondestructive testing. He was one of the primary technical contributors to the early SAFT work at Battelle. From 1984 to 1987, he was an Assistant Professor of Radiology at the University of Cincinnati, where he was instrumental in the development of a research oriented MR imaging facility. There, he worked primarily on image reconstruction methods specific to MR imaging with perfluorocarbon compounds. He worked briefly as a Project Leader for General Electric-Aircraft Engines in Cincinnati and then joined TETRAD Corp., first as a consultant and later as Senior Scientist. His current research interests are focused on methods for intravascular and interventional ultrasound imaging and Doppler. Of primary concern are novel transducer configurations and imaging methods.

Dr. Busse is a member of the American Association of Physicists and the Society of Magnetic Resonance in Medicine.